JOURNAL OF MATERIALS SCIENCE **34** (1999) 1959–1972

Influence of ceramic powders of different characteristics on particle packing structure and sintering behaviour

DEAN-MO LIU*‡, JIANG-TSAIR LIN
Materials Research Laboratories, Industrial Technology Research Institute, Chutung, Hsinchu, Taiwan 31015

Ytteria-stabilized zirconia powders from different sources were used to investigate powder packing characteristics and subsequent sintering behaviour. Powders of different levels of agglomeration were controlled by varying degrees of ball-milling, followed by shaping through colloidal casting. Experimental findings revealed that the average pore diameter of the powder compacts appears to be a good representative of the whole pore structure of the green compacts. This pore parameter exhibited a well-defined correlation with respect to the initial mean powder size for each type of powder, irrespective of the difference in particle size distribution and degree of agglomeration, and also correlated soundly with the sintering behaviour of the powder compacts. Critical pore diameter/particle size ratios were experimentally determined, which were shown to be strongly related to the initial particle size by a power-law dependence. This dependence offers an excellent prediction of the critical ratio in alumina powder compacts reported by Zheng and Reed [27], which further supports the feasibility of this relationship.

1. Introduction

Dense, fine-grained technical ceramics with chemically and physically uniform microstructures are always favourable for providing desired properties to meet diverse engineering applications. To achieve ceramic products with a uniform, dense, and fine microstructure, a ceramic powder compact with high green density is important and this has been an interesting subject of many publications [1–7]. A number of papers have particularly emphasized the significance of pore size distribution on the sintering behaviour and end-point density of the ceramics. A quantitative observation by Dogan *et al.* [8] and Roosen and Hausner [9] indicated that pore size distribution is directly reflected in the relative position of the shrinkage rate curve. Roosen and Bowen [10] have used most frequent pore diameter (the maximum frequency on volume-pore diameter spectrum obtained through a mercury instrusion technique) to represent the whole pore structure of the green compact and to correlate subsequent sintering phenomena; however the resultant correlation was poor.

Recent communication by the present author [11, 12] have found that the average pore diameter (APD) determined by 4-fold pore volume divided by pore surface area provided a well-fitted linear correlation with respect to green density of the powder compacts made from a powder injection molding technique. A similar observation was also found by Halloran *et al.* [13] in the study of alumina powder consolidated by die-pressing. These findings provides a strong indication that APD is likely to act as a true representative of the whole pore structure for a given uni-modal particle packing structure (we presently do not realize how it works on a multi-modal particle packing structure). In the current investigation, a colloidal casting route was employed to consolidate powders from different sources, representing different particle size and shape, sinterability, and degree of agglomeration. The green as well as the sintered density at different stages of sintering of the powder compacts was characterized in terms of the APD to examine how these properties are related to the pore structure. In this investigation, an attempt is made to correlate the particle packing structure with the given nature of powders under identical process control. It aims to provide some understanding on how the powder nature affects the particle packing structure.

In most powder compacts, particles (with some agglomerates) are randomly packed to developed a spectrum of pore size; some of them are relatively large with respect to the individual particles (usually refer to as inter-agglomerate pores) and some are small (e.g., intra-agglomerate pores). The large pores are frequently residual within the ceramic body even at the final stages of sintering and eventually reduce end-point density

* *Current address*: Department of Materials Science and Engineering, University of Pennsylvania, 3231 Walnut Street, Philadelphia, PA 19104, USA.
‡ Author to whom all correspondence should be addressed.

[4, 14, 15]. The elimination of pores is a critical process of sintering. Kingery and Francois [16] were the first to indicate the importance of the pore coordination number (i.e., the number of particles or grains enveloped a pore) for pore elimination. They indicated that pores larger than some critical ratio (i.e., pore diameter/particle size ratio) would survive even until the final sintering stage. Only those below the ratio are thermodynamically unstable and would be completely eliminated. Lange [17] further outlined the re-distribution of the pore coordination number towards a smaller value by both increases powder consolidation force and grain growth during sintering. Both effects enable the enhancement of end-point density. However, the latter route would result in microstructural coarsening which is undesirable in practice. More recently, Zheng and Reed [18] conducted an experiment by preparing a series of alumina powder compacts with different pore size distributions. They observed the change of the pore size distribution during various stages of sintering and found that pores smaller than half of the initial mean particle size (D) were eliminated and determined the critical ratio to be 0.5. They further proposed a pore elimination map by classification of the pores into micropores (with size $<0.5D$), macropores ($>10D$), and coarse micropores (between $0.5D$ and $10D$). Those pores categorized as macropore could not be eliminated and should be avoided during powder consolidation. More complicated pore elimination/growth mechanism were observed for coarse micropores. In principle, the finer the pore structure inside the green compacts, the easier the pore elimination.

No experimental findings or theoretical expectation have mentioned how particle size (or degree of agglomeration) affects the pore coordination number and how it influences endpoint density. This is probably due to lack of more systematic investigation on using powders covering a wide range of particle size (and a range of agglomeration levels), representing different degrees of sintering activity. In this study, five ceramic powders with mean particle size ranging from 0.08 to 0.5 μm were employed. This range of the mean particle size represents widely-used powders that appear in practical fine ceramic processing. A mathematical relationship was derived experimentally to correlate the critical ratio with the corresponding particle size based on the analysis of residual fractions of pore of varying sizes within the green compacts after the final stage of sintering.

2. Experimental procedures

Five commercially available zirconia powders (designed as powder A, B, C, D, and E) were used to form powder compacts by means of a colloidal casting route. All the powders contain 3 mol % Y_2O_3 as stabilizer. Impurity content of the powders is given in Table I. The powders were dispersed into aqueous media with 0.5 wt % dispersant and 1 wt % plastisizer in a polyethylene jar containing a fixed powder-to-zirconia ball (as milling media) weight ratio. The suspension was mixing for different periods of time from 0.5 h to as long as 72 h, followed by casting into a rectangular-shaped plaster mold to consolidate a shape. The powder compacts were then oven-drying and subjected to slow pyrolysis to 600 °C for 2 h to eliminate residual organic phases. The particle size distribution of the powders after different periods of time of ball milling was characterized using a particle size analyzer (Horiba, LA-910, Japan). A small portion of the powders was further diluted and ultrasonically dispersed, followed by examination using scanning electron microscopy (SEM, Cambridge Instruments, Model 360) to determine the size and the shape of individual particles. The specific surface area of the as-received powders was determined using an isothermal nitrogen adsorption technique.

TABLE I Impurity content (wt %) in the 3 mol % Y_2O_3-stabilized zirconia powders

Ingredient	Powder A	Powder B	Powder C	Powder D	Powder E
CaO	0.02			0.02	
Na_2O	0.01	0.01			
Fe_2O_3		0.02	<0.002	0.04	0.003
SiO_2		0.05	<0.002	0.03	<0.001
Na_2O		0.01	0.025		0.015
TiO_2		0.01		0.15	0.006
Al_2O_3			<0.005	0.02	<0.003
S				0.05	
L.O.I[a]	0.14	0.5	0.81		0.26

[a] Loss of ignition wt % at 1100 °C.

The green compacts were characterized using mercury porosimetry (Autopore II 9220) for pore size distribution. The particle packing structure is examined using the SEM. Although several assumptions have been made for pore size measurement, the porosimetry undoubtedly is still a useful tool for a better understanding of the packing structure within a green compact. Powder compacts were cut into cubes of dimensions $5 \times 5 \times 5$ mm^3 and companion-fired under a constant heating rate of 5 °C/min to temperatures of 1200 to 1500 °C with an increment of 100 °C. The sintered densities of the fired compacts were then measured using the Archimede's principle with water as a medium.

3. Results and discussion

3.1. Powder characterization

Figs 1a–e show the morphology of the as-received powders for powder A, B, C, D, and E, respectively. Except that of powder D having an irregular shape, the rest of the powders are relatively fine and exhibit near-spherical shape. The mean particle size of the powders was determined by averaging over 500 individual particles, together with their specific surface as listed in Table II. Powder Has the smallest particle size, about 0.08 μm and powder D, the largest size, 0.5 μm. One common observation of these powders is the presence of agglomerates (no attempt is made to differentiate agglomerates and aggregates here) and it is generally accepted that the smaller the particles, the greater extent of agglomeration due to stronger interparticle attraction/adhesion forces.

The purpose of ball milling for different periods of time was to intentionally introduce agglomerates of

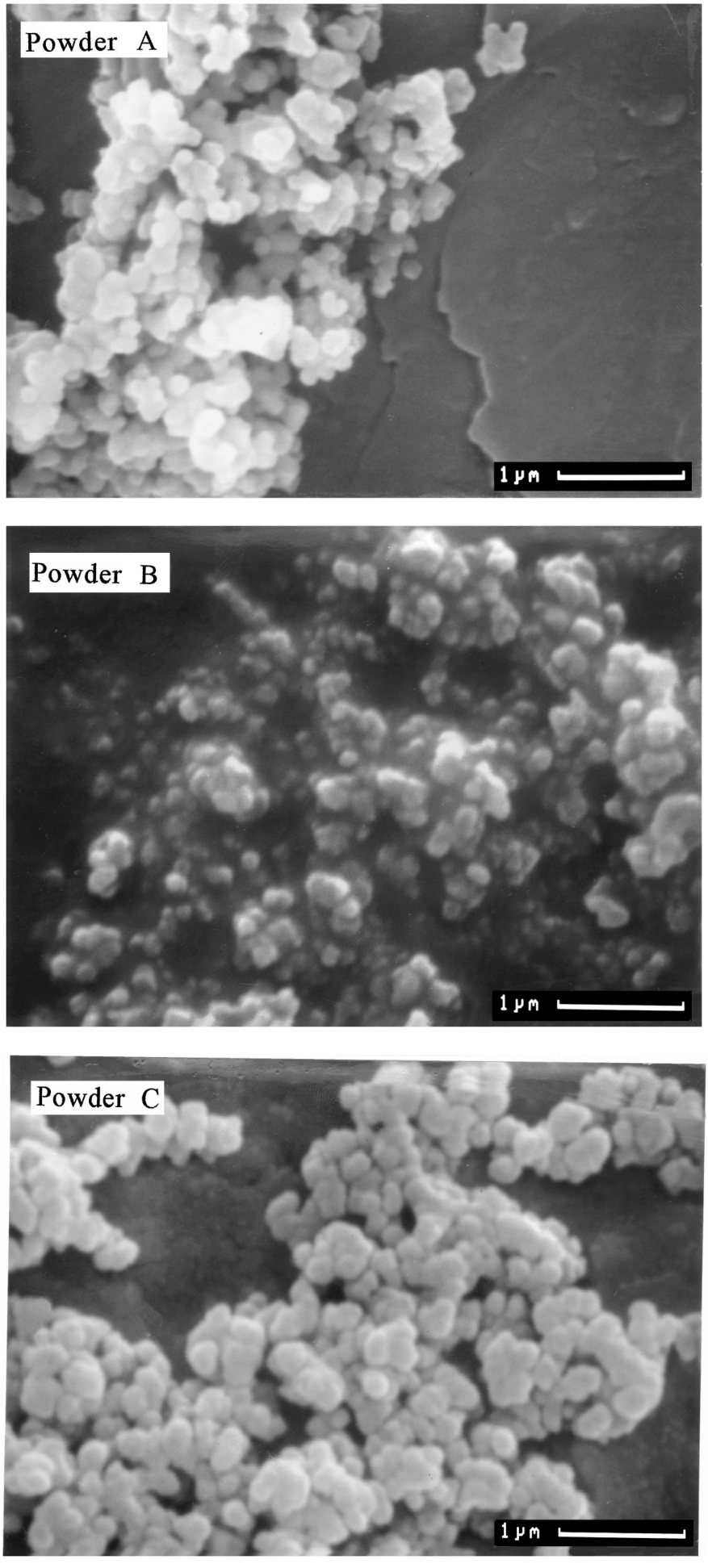

Figure 1 Scanning electron micrographs of ZrO_2 (a) powder A, (b) powder B, (c) powder C, (d) powder D, and (e) powder E, used in this investigation.

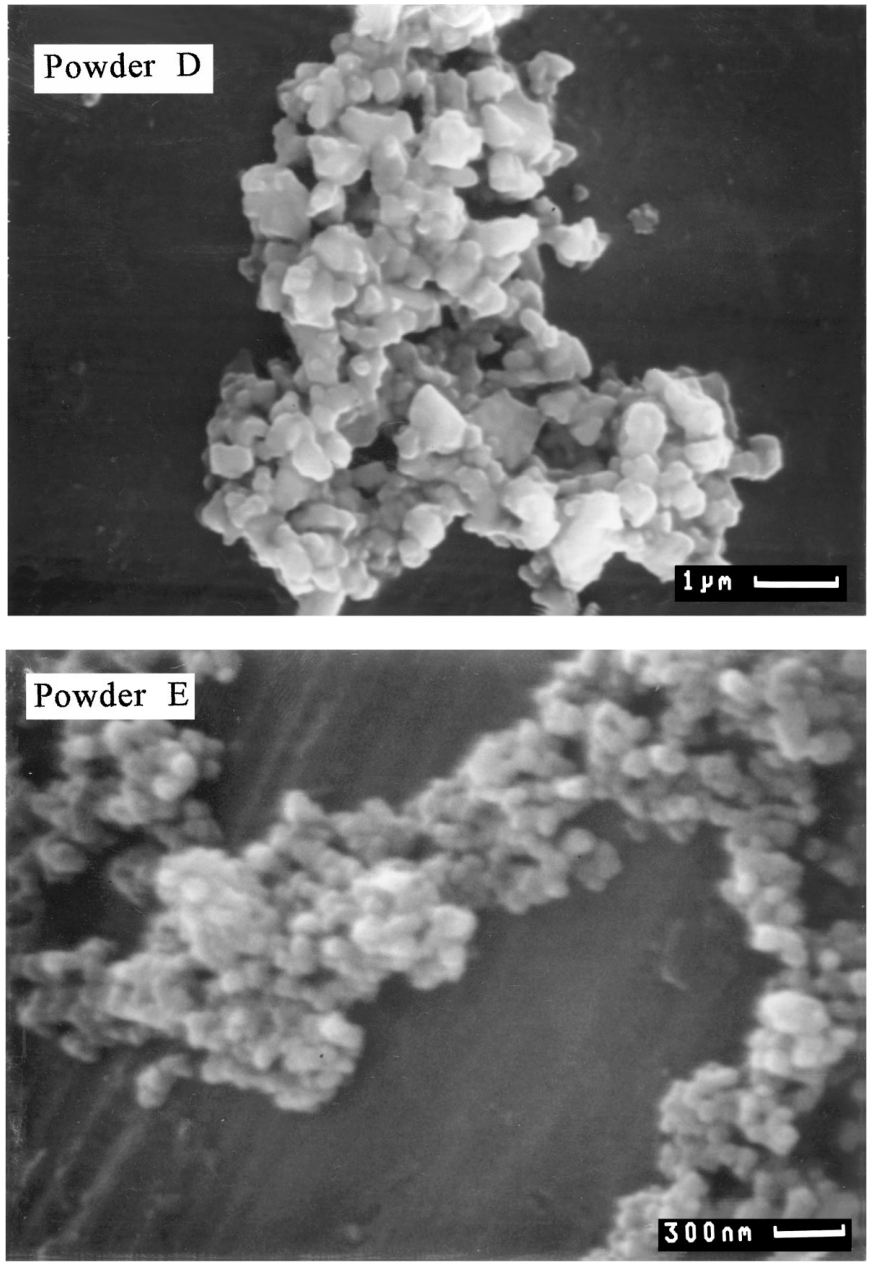

Figure 2 (*Continued*)

different levels. Fig. 2 shows the particle size distributions (here we use the legend *agglomerate size distribution* which is preferable as an expression of the true powder condition) of the powder A after different time periods of ball milling. As time proceeds, the size distribution shifts to a smaller region indicating the breaking of agglomerates. A reduction of individual particles by the grinding ball crushing is also possible, but should be relatively small portion simply because the ball size is large (20 mm in diameter) in comparison to the powder size. This size of ball media is usually not used for particle size reduction, particularly for submicron-sized powders, in practice.

In comparison to the visually-determined individual particles, the volume-averaged mean agglomerates are much greater in size and agglomerates with a mean size of as large as 10-fold mean particle size as observed for powder E, suggesting extensive agglomeration. To quantify the degree of agglomeration of the prepared powders, an expression termed agglomeration parameter introduced by Roosen and Hausner [9] by defining a ratio of median agglomerate size to the corresponding particle size was used and the resulting ratio is also given in Table II. The higher the ratio indicates the greater extent of agglomeration and it is clear that powder E (having the smallest particle size) possesses the most extensive agglomeration, whilst the powder D is considered to be well-dispersed.

3.2. Particle packing characteristics

Lange [19] indicated that colloidal processing provides improved particle packing efficiency in comparison to the conventional die-processing route. For a well-dispersed colloidal suspension, the particles can be slide over one another to pack with high efficiency and a relatively high green density can usually be obtained. However, agglomeration reduced packing efficiency, which further coarsens and broadens the resulting pore size distribution of the green compacts.

TABLE II Some parameters, i.e., specific surface area (SSA), agglomeration parameters (AP), and green density (%TD), of the zirconia powders used in current investigation

Materials	SSA (m^2/g)	AP (milling hour)	Green density
Powder A		5.45[b] (0.5 h)	43.51
(0.20 μm)[a]	7.16#	4.97 (8 h)	45.02
		4.66 (16 h)	48.14
		4.1 (24 h)	52.61
		3.44 (48 h)	54.25
Powder B		3.95 (0.5 h)	45.35
(0.32 μm)	7.06	3.06 (8 h)	51.52
		2.36 (24 h)	54.89
Powder C		2.35 (0.5 h)	47.80
(0.23 μm)	6.32	2.17 (8 h)	51.82
		1.86 (24 h)	53.90
		1.75 (48 h)	54.83
Powder D		2.35 (0.5 h)	47.83
(0.5 μm)	6.64	1.35 (8 h)	51.82
		1.26 (24 h)	53.36
Powder E		11.08 (0.5 h)	42.05
(0.08 μm)	15.01	7.20 (24 h)	44.35
		5.67 (48 h)	46.22
		5.20 (72 h)	46.76

[a] SEM-determined mean particle size. # BET nitrogen adsorption determined.
[b] Values are determined by dividing the mean agglomerates size with the mean particle size.

Figs 3a and b illustrate the pore size distribution of the compacts with powders ball-milled for 0.5 and 24 h, respectively. A relatively small portion (<2 vol %) of pores greater than 1 mm is detectable (not shown in these figures) and these pores should be taken as interagglomerates voids. It is clear that agglomerates break apart extensively during long-term ball-milling into smaller fragments (either agglomerates or individual particles, or both), these fragments tend to be kept apart by the organic dispersant in the powder suspension. This dispersion facilitates fragments sliding over one another upon casting and improves particle packing efficiency, resulting in a higher green density (Table II). Furthermore, a smaller and somewhat narrower pore size distribution (Fig. 3a) can be developed within the green compacts when smaller particles were used (e.g., powder E), in spite of having a maximum agglomeration and a minimum green density (42% of theoretical). Since agglomeration should deteriorate the green microstructure of the powder compacts by coarsening the pore size distribution, the observed agglomeration versus corresponding pore size distribution for powder E compact contradicts such understanding. This may be attributed to having originally the finest particles. Extensive agglomeration produces agglomerates with a means size (0.5–0.7 μm) still smaller than those produced by others (0.8–1.4 μm).

Accordingly, increase in powder agglomeration reduces green packing density. This can be confirmed by a correlation of the relative green density with agglomeration parameter defined previously (Fig. 4). The coefficient of the correlation has a low value of 0.680; however, the trend of decreasing green density with increasing degree of agglomeration is evident. The relative green density would reach ~58% once the powder is perfectly dispersed, i.e., agglomeration parameter is unity or particles are finely-divided.

Alternatively, each powder may be treated separately as its own agglomeration-density relation and extrapolation to the "perfectly-dispersed" density results in a value ranging from 58 to 68% theoretical. The 58% density obtained is identical to those computer-simulated results obtained by Rodriguez *et al.* [20] and Visscher and Bolsterli [21], and also comparable with theoretical value derived by Dixmier [22] for packing of identical spheres. However, it would be more realistic in considering the finely-divided particles (if perfectly dispersed in the liquid media) to be a continuous

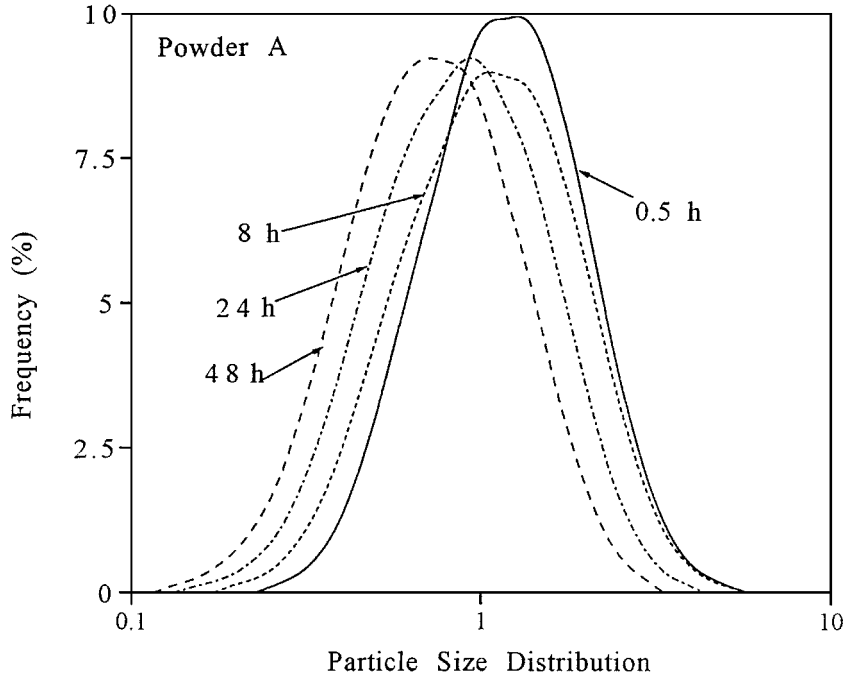

Figure 2 Particle size distributions of the powder A after different time periods of ball milling.

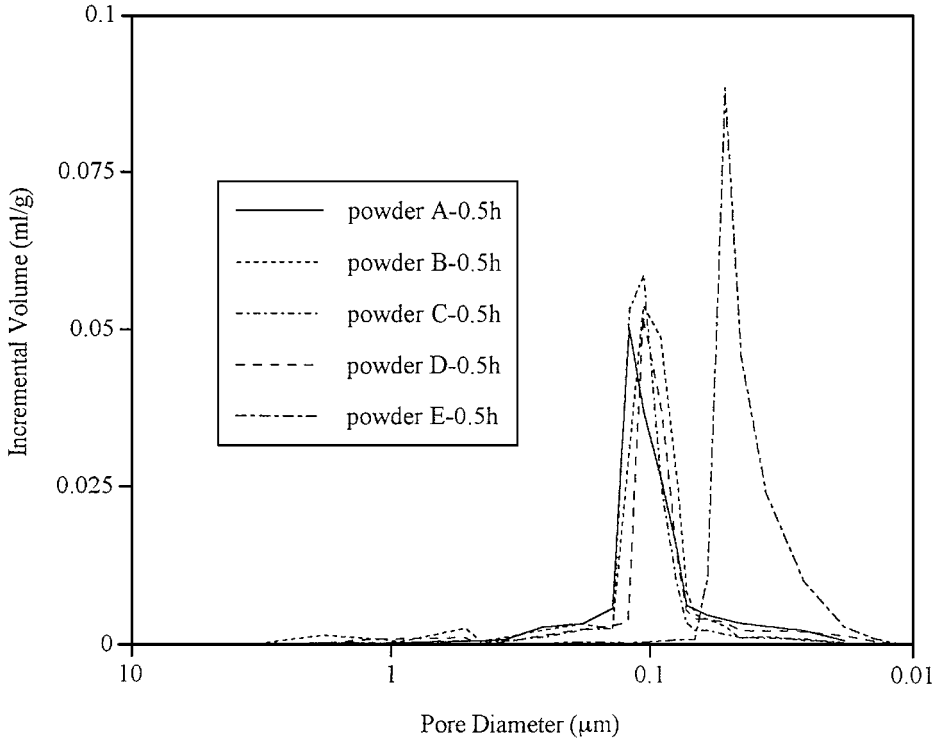

(a)

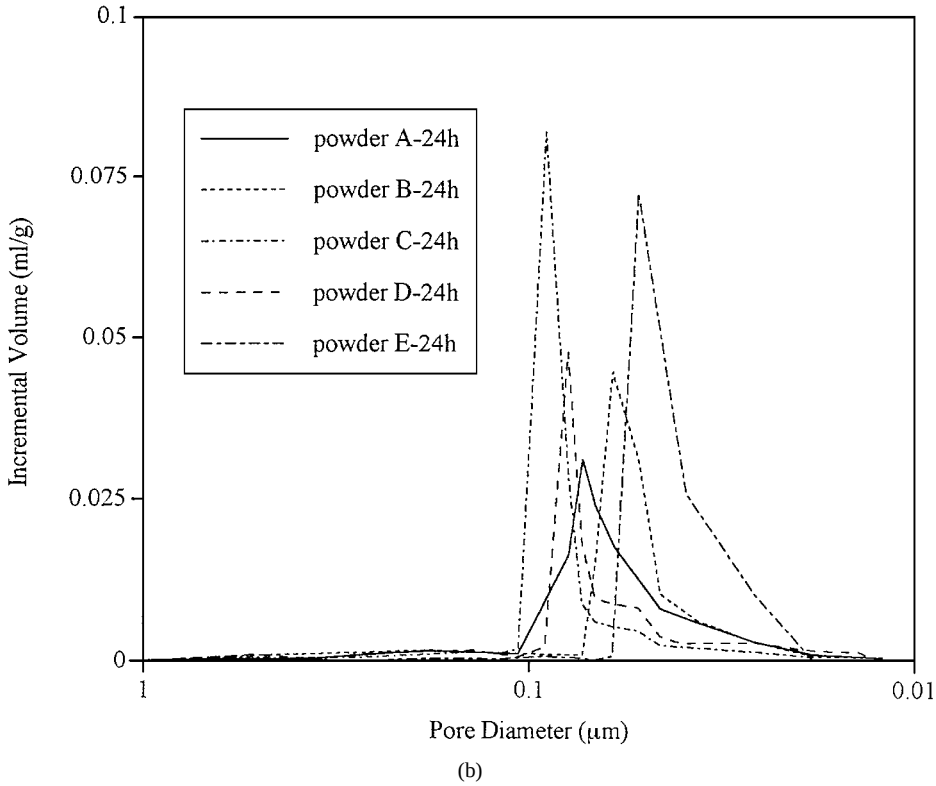

(b)

Figure 3 Pore size distributions of the green compacts of different powders after (a) 0.5 h and (b) 24 h of ball milling.

distribution of size (i.e., log-normal dispersion, in Fig. 2). Such a normal particle size distribution is theoretically able to produce a compact of spheres with a dense random packing density over the range of 59–63%. The currently-obtained value is apparently lower than the theoretical expectation and is evidently a "loose random packing" structure. The non-spherical particles currently used may be one of the possibilities responsible for such discrepancy. In comparison, the extrapolated "well-dispersed" green density is considerably lower than that for fine-particle Al_2O_3 [2, 10], 65% or above, and SiC [23], 68%, obtained under a similar consolidation route. Accounting for such differences in packing density among those powders would be complex and is beyond the scope of the current investigation.

The use of the concept of the *most frequent pore diameter* originated by Roosen and Bowen [10] to correlate the pore structure with the resulting green density is highly uncertain. Instead, the average pore diameter is

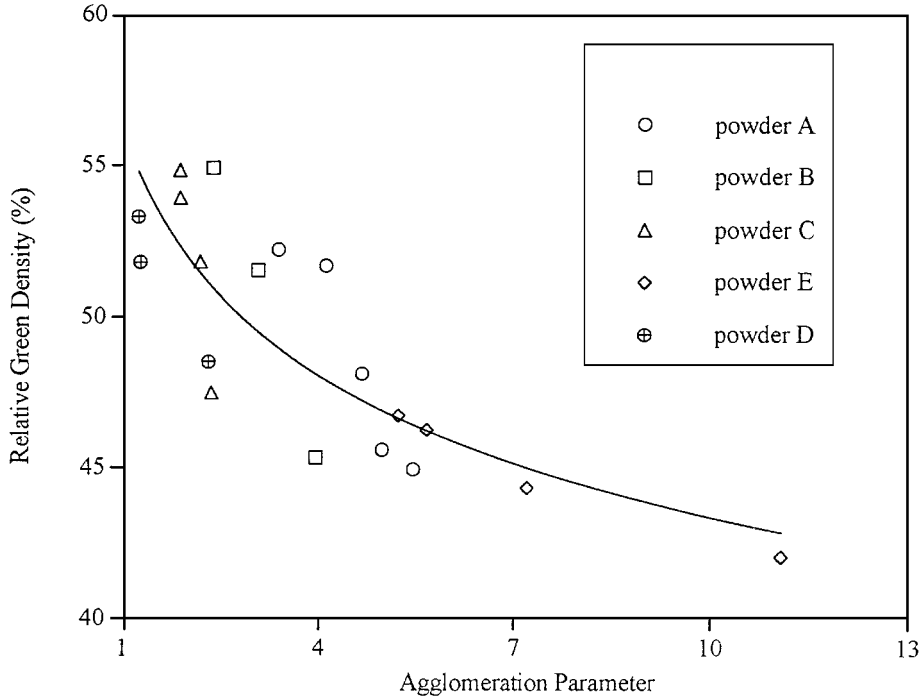

Figure 4 Correlation between the green densities of the powder compacts and agglomeration parameter for various powder characteristics, showing roughly identical trend with which the packing density reduces with increasing degree of powder agglomeration.

likely to provide somewhat more useful and reliable parameter in describing the green property of the powder compacts. Expressing the average pore diameter (APD) of the powder compacts containing varying degrees of agglomeration in terms of the green density is shown in Fig. 5. Each powder presents a well-fitted linear relation with correlation coefficient ranging from 0.97 to 0.99. Each powder has its own linear APD-density relationship, indicating the uniqueness, such as particle size/shape and degree of agglomeration, of the powders. This also provides some clues in understanding the fact as depicted in Fig. 4 that each powder may exhibit its own packing characteristic. In general, a greater APD is obtained in the powder compact with higher agglomeration (i.e., compacts with lower green densities).

Since a well-defined correlation can be established between APD and green density of the powder compacts, it may be of considerable interest to determine whether a particle or agglomerate parameter can be related to the corresponding pore structure. In an average sense, as previously defined for representation of the pore structure, a mean particle or more realistically a mean agglomerate size (determined by the particle size analyzer) was tentatively selected as a powder parameter under a given condition of agglomeration. Surprisingly, a straight line can be obtained by correlating

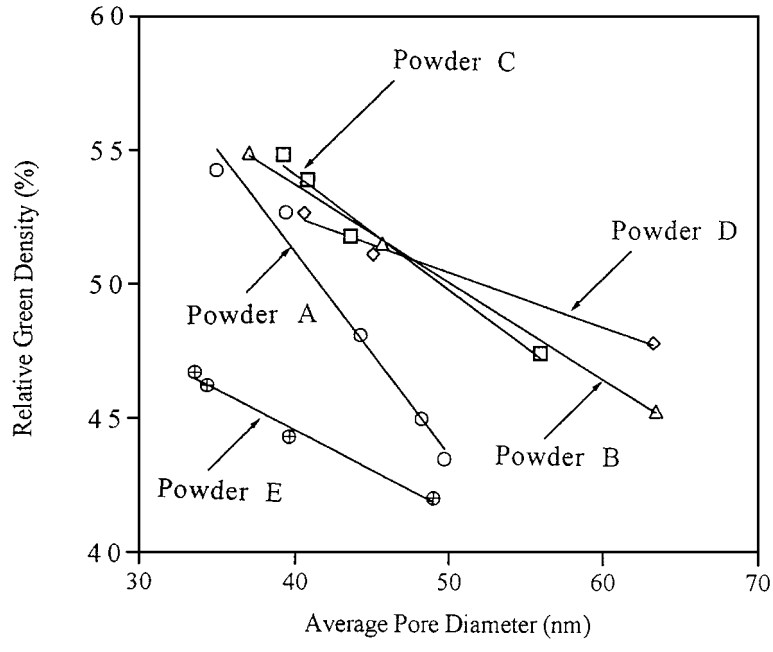

Figure 5 Correlations between average pore diameter and packing density, showing an excellent agreement with respect to each type of powder.

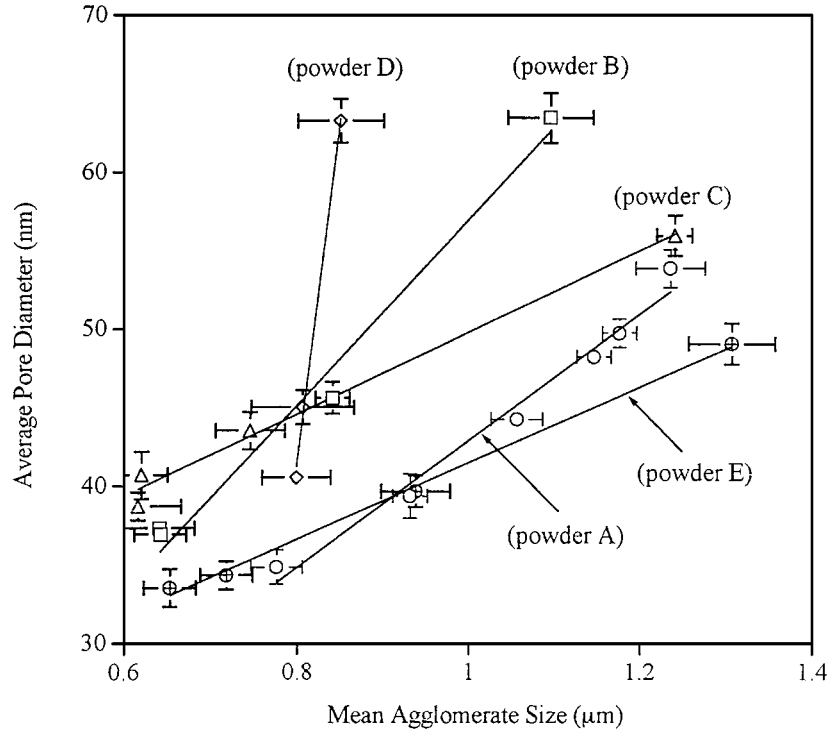

Figure 6 Good correlations are obtained between mean agglomerate size and average pore diameter for each type of powder, suggesting the presence of a simple relationship between them under colloidal processing.

the APD with the mean agglomerate size for each type of powder as shown in Fig. 6. The error bars in this figure are referred to as the standard deviation of the measurements. For a given powder, the resulting particle packing structure changes linearly with powder condition, or implicitly, with the degree of powder agglomeration. The small measurement deviations indicate that a highly reproducible packing structure was achieved by means of the colloidal casting technique and this ensured a reasonable uniformity of sintered microstructure under proper suspension control [19]. This powder characteristic-related packing structure observed presently is suggested to be a result of the nature of the consolidation method because the suspended small fragments would be likely to deposit, under both gravity and suction force (by the plaster mold) fields [24], particle by particle and layer by layer. Such consolidation mechanisms (being physically similar

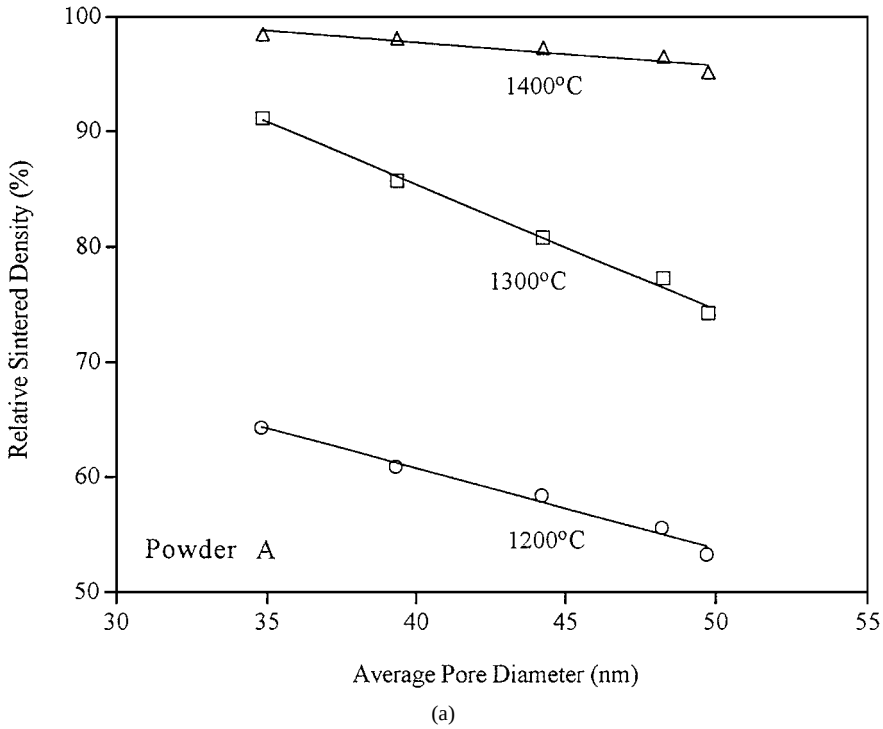

(a)

Figure 7 Average pore diameter versus relative sintered density for (a) powder A, (b) powder D, and (c) powder E, at temperatures of 1200–1400 °C, corresponding to different stages of sintering. This also illustrates that the average pore diameter is a fairly good pore parameter in describing the sintering behavior of the ceramic powders currently employed.

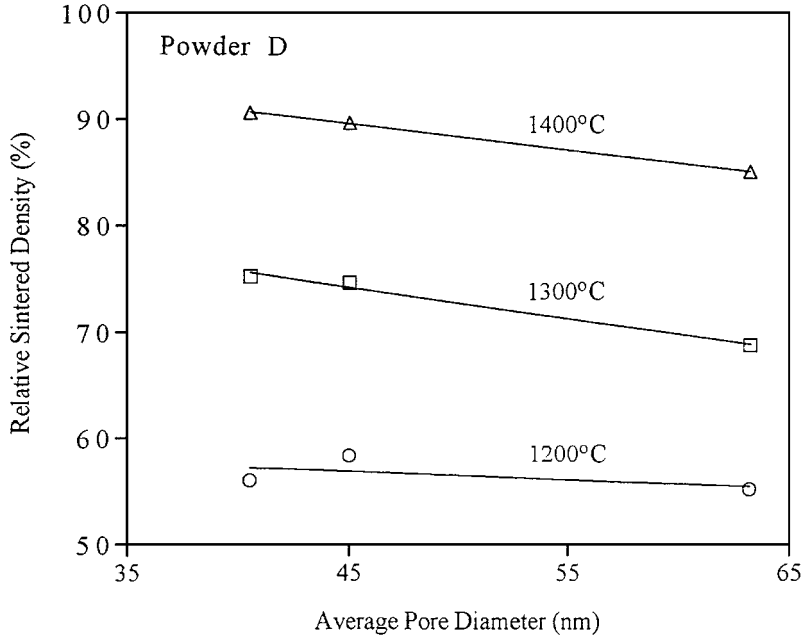

(b)

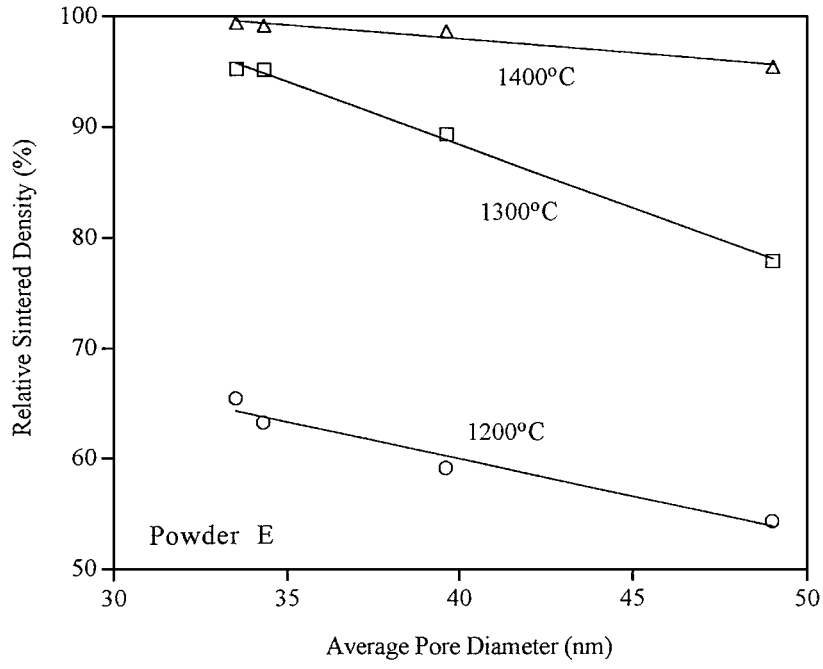

(c)

Figure 7 (*Continued*)

to the method for theoretical models and simulation previously mentioned) ensure the reproduction of particle packing pattern (or structure) to a significant extent and this renders the final packing structure to be directly related to the starting powder characteristics. No identical physical conditions can be obtained between different powders and this roughly reflects their unique features in the final green packing structure produced via colloidal casting.

3.3. Influence of particle packing characteristics on sintering behaviour

Roosen and Bowen [10] attempted to use the *most frequent pore diameter* to correlate the sintering behaviour of alumina compacts but this resulted in a relatively poor correlation. In our opinion, their selection of the *most frequent pore diameter* as a representative of the whole pore structure of the green compact is incorrect, primarily because powder compacts can have identical *most frequent pore diameter* but large difference in pore size distribution. This can be evidenced by Fig. 7 in [10]. In contract, the APD presently used reflects, in considerably certainty, the whole pore structure of the green compacts and is likely to be sensitive to a slight microstructural variation.

Based on this understanding, together with the observation of shrinkage rate curve versus pore size distribution previously mentioned [8, 9], it is reasonable to hypothesize that the sintering behavior of a given powder compact may be able to be correlated with the APD of the compacts. The resulting relations are evident

as shown in Figs 7a, b, and c for powders A, D, and E, representing particles of intermediate, the largest, and the finest size, respectively, which yields a linear relationship for each powder at different temperatures from 1200 to 1400 °C. These temperatures involved a wide range of sintered density covering different stages of sintering (mostly intermediate-stage sintering). The correlation coefficients over these straight lines are in the range of 0.91–0.99 indicating the sintering behaviour is able to follow a linear function of the APD of a given green compact.

The negative slopes of these lines along with the increment of the APD indicate that agglomerates suppress densification [4, 25, 26]. Such suppression becomes stronger for smaller particles (e.g., powders A and E) at lower temperatures (1200–1300 °C) and for larger particles at higher temperatures. This is primarily because the smaller-particle constructed agglomerates have priority densification at lower temperatures and their densification effect becomes less pronounced for powders of higher content of agglomerate [25]. This finding implies that it is relatively difficult or impossible to determine the sintering parameters with accuracy between various powder compacts without considering the effect of agglomeration, even if they have initially identical packing density.

Taking powder E as an example, the influence of agglomerates on sintering behaviour can be expressed by using the term "sintering activity" defined as the ratio of $(D_s - D_g)/(100 - D_s)$, where D_g is the green density and D_s the sintered density, as previously used by Roosen *et al.* in the study of ZrO_2 powder [9]. Fig. 8 shows the relations between the sintering activity and corresponding sintering temperature for powder E with different degrees of agglomeration (expressed as "agglomeration parameter" in parentheses). Apparently, the lower the degree of agglomeration, the higher the sintering activity results and such sintering behaviour appears to be sustained over almost the entire length of sintering. Such an agglomeration-dependent sintering behaviour imposes a profound effect on sintering kinetics as recently observed and will be discussed in detail separately. A potential risk in determining sintering parameters such as activation energy, densification/shrinkage, diffusion activity, etc., with certain quantitative error would probably arise.

According to the complex model of pore elimination map proposed by Zheng and Reed [18], pores smaller than half of the mean particle size (D) can be totally eliminated; however, pores greater than $0.5D$ can be either shrink or grow, and those greater than $10D$ can not be eliminated. Therefore, the pore stability with most uncertainty is the size over the range of $0.5D$–$10D$. However, no further investigations are available in providing deeper understanding on (1) How pores "behaves" over this large range of size? (2) Is there any influence of starting particle size on the critical ratio? (3) Has any "critical pore size" existing in a powder compact? (4) Is such a pore classification may applicable to other ceramic powder compacts other than alumina?.

To elucidate these questions, we first examined the total residual porosity of all the compacts after the final-stage sintering. T_{NS}, the temperature at the final stage was determined when no further shrinkage was detectable on the dilatometer and a few samples exhibiting a temperature beyond the maximum temperature attainable of the instrument were abandoned. This total residual porosity can be expressed as a sum of the fractional porosity (P) of different pore size regimes, which yields,

$$P_{\text{green}} = P_{\text{macropore}} + P_{\text{transition pore}} + P_{\text{micropore}} \quad (1)$$

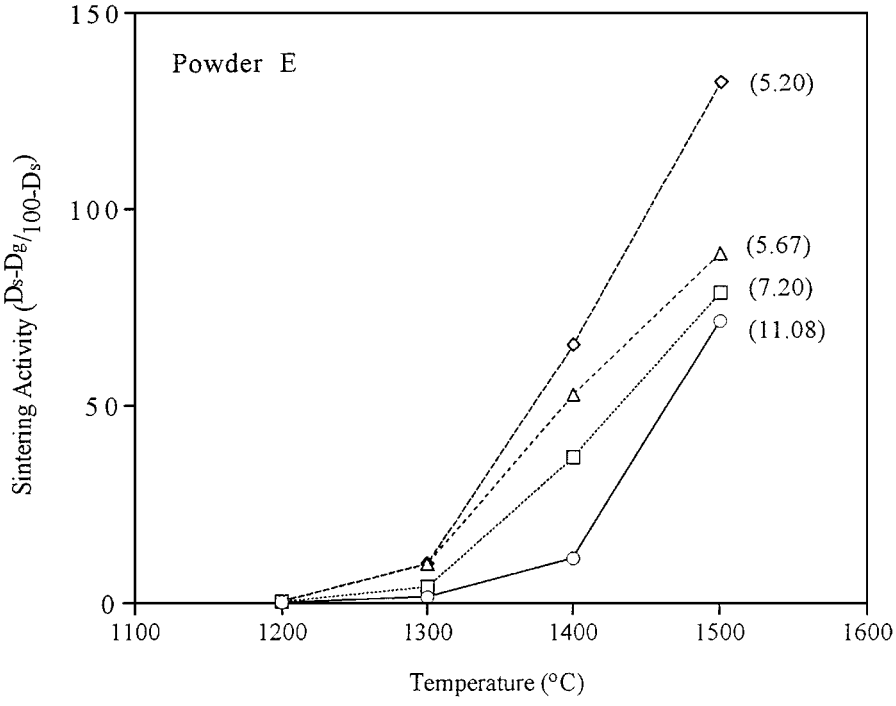

Figure 8 The sintering activity of powder E with different degrees of agglomeration (values in parentheses are "agglomeration parameter") with corresponding sintering temperatures.

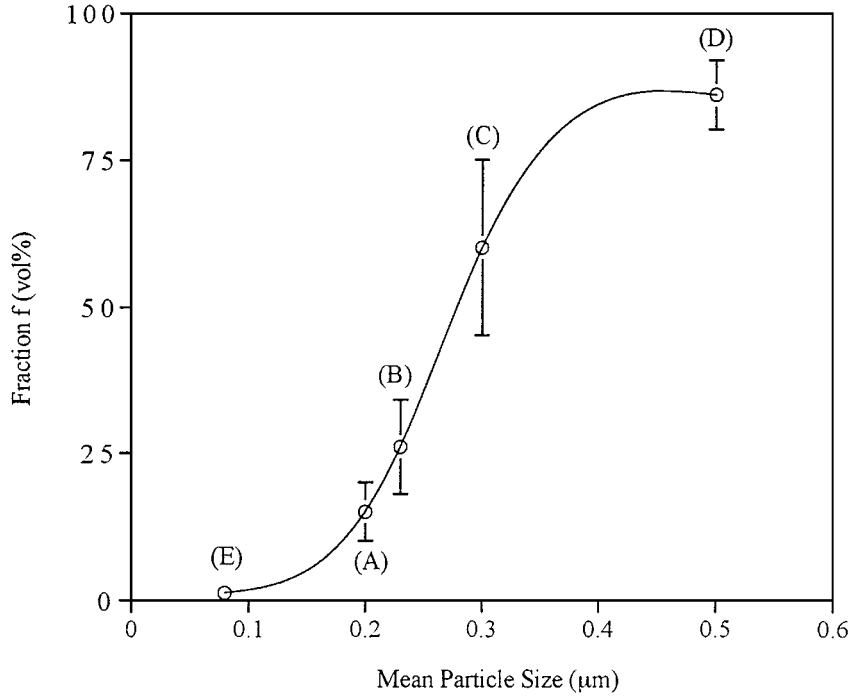

Figure 9 The volume fraction f as a function of mean particle size.

The meaning of the transition pore will be defined in a later discussion. The T_{NS} is dependent on powder characteristics and is over the range of 1460–1540 °C for the powders currently used. According to the observation of Zheng and Reed [18], the porosity of the large pores (defined as the macropores, $>10D$, in their article) in the green stage is nearly identical as in the sintered stage, that is,

$$(P_{\text{macropore}})_{\text{green}} = (P_{\text{macropore}})_{\text{sintered}} \tag{2}$$

If Equation 2 continues to the final stage of sintering (in fact, from a recent observation on an other ceramic system with relative large pores, Equation 2 sustains until the final-stage sintering [28, 29]), it provides important and useful implication in how the pores with size over the range of $0.5D$–$10D$ undergo morphological changes (here we define these pores as transition pores).

In comparison, the residual porosity of the compacts is always greater in different quantities that the porosity of the macropores, i.e.,

$$P_{\text{residual}} = P_{\text{macropore}} + P' \tag{3}$$

Based on the pore elimination map [18], we believe that some transition pores should grow or remain unchanged rather than shrink to final elimination and they contribute to the residual porosity. This leads to a need for further analysis of how much volume fraction (f) of the transition pore for these powder compacts turns into the region of macropore. That is to say, some fraction of the transition pores in fact undergoes relatively unchanged morphologically (i.e., thermodynamically stable pores) and can roughly be categorized as macropores. Equation 3 can then be rewritten by,

$$P_{\text{residual}} = P_{\text{macropore}} + f\,P_{\text{transition pore}} \tag{4}$$

The determination of the fraction f is then to be particularly important in providing a more detailed understanding of how the pores undergo morphological change during sintering. Following the analysis of the pore size distribution, we found that the fraction f tends to increase with an increase of the particle size; for instance, $f = \sim$1–1.5% for compacts made from powder E and over 80% for powder D compacts. A plot of the fraction f in terms of the initial particle size is shown in Fig. 9, where the bars refer to as the minimum and maximum fraction f. The trend of fraction f in relation to the particle size is evident. This finding provides a strong implication that some critical ratio must be existing in the transition pore region. To be more specific, pores below $10D$, e.g., $7D$, $8D$, etc., undergo similar change (or unchanged) as that of $10D$ pores and those above $0.5D$, e.g., $0.8D$, $1D$, $2D$ etc., may be totally eliminated as that of $0.5D$ pores. This argument in fact does not show any conflict with the concept of pore coordination number outlined by Lange [17] and will be discussed later.

Hence, such critical ratio is not supposed to be independent of the starting particle size. Returning to the initial volume-pore diameter data, a specific pore size corresponding to approximately the fraction f for the respective powder can be determined. Such pores always lie in the range of the transition pore region, but exhibits a different size value, depending on the starting particle size. Dividing the obtained specific pore diameter with the starting mean particle size, a new definition of the critical ratio is obtained. Plotting the critical ratio with respect to the mean particle size, a power-law expression (solid line in Fig. 10) with correlation coefficient as good as 0.96 yielded:

$$\text{Critical Ratio} = 0.289D^{-1.17} \tag{5}$$

where D has a unit in μm. Equation 5 is applicable to the

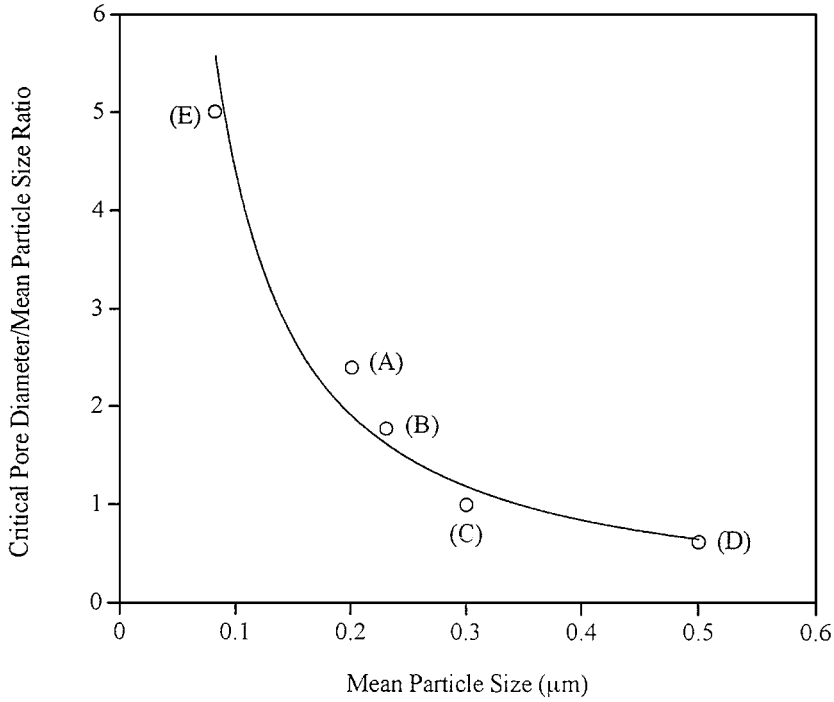

Figure 10 The critical (pore diameter/particle size) ratio shown to be inversely proportional to power-law dependence of starting mean particle size over the range of 0.08 to 0.5 μm.

ceramic system currently investigated with the particle sizes over the range of 0.08 to 0.5 μm, which cover the size of most commercially available ceramic powders for technological applications. Since Equation 5 is deduced experimentally from examination of the particle packing structure in relation to the solid-state sintering, it is therefore possible to extend this equation to other similar systems and to see how this equation works. Available data for critical ratio determination are relatively rare, but an earlier work by Zheng and Reed [27] is used. Their model material is alumina powder having a mean particle size of 0.64 μm. The critical ratio is calculated to be 0.49 from Equation 5 which is in excellent agreement with their experimental observation, 0.5. This comparison, in spite of a slight extrapolation to a larger particle size than the studied range, supports the validity of Equation 5.

Equation 5 indicates the strong dependence of the critical ratio on the starting particle size, which has not been reported in literature. This finding appears to be explicable in terms of the concept of pore coordination number. Since it is realized that grain growth has the potential to reduce pore coordination number, this accelerates pore elimination and improves end-point density

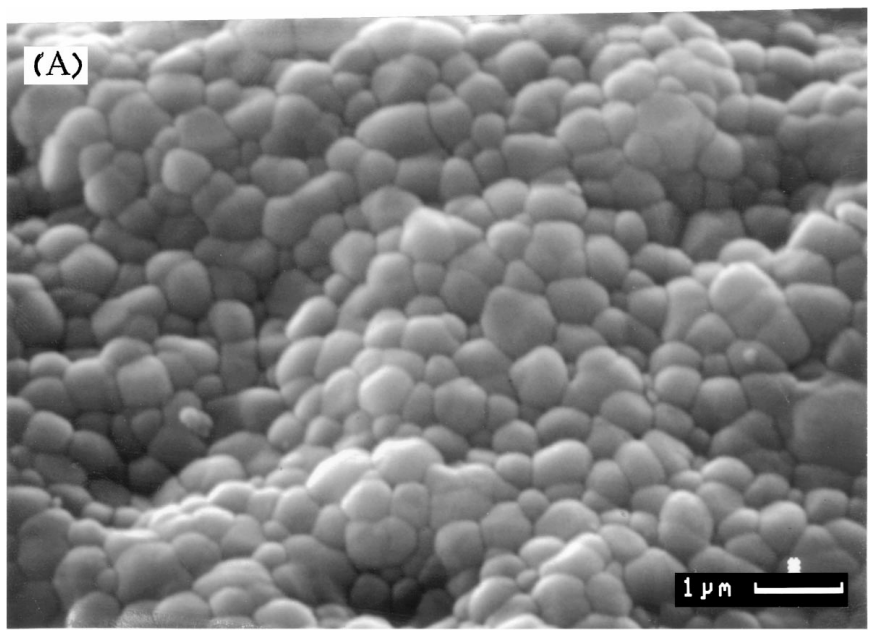

Figure 11 The sintered compacts made from (a) powder A, (b) powder D, and (c) powder E, shows different microstructural evolution at T_{NS} with grain size of 0.5, 0.75, and 0.35 μm, respectively, which indicates a significant grain growth occurring for smaller particles.

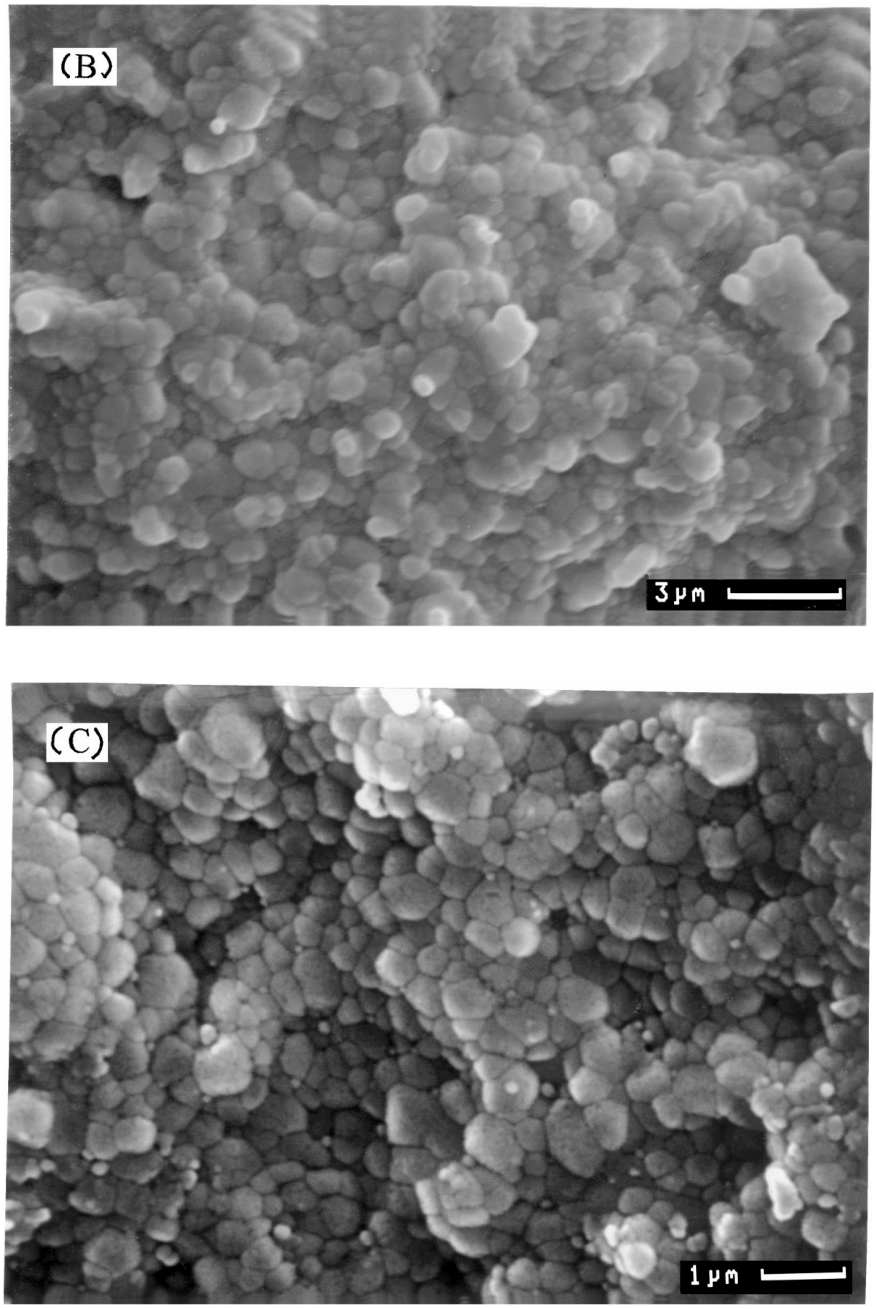

Figure 11 (*Continued*)

of the ceramic bodies. The use of smaller particles has the greater tendency for grain growth (also for densification) than larger ones; this may promote the reduction of pore coordination number. A sintered microstructure for powders A ($T_{NS} = 1510\,^{\circ}C$), D ($T_{NS} = 1540\,^{\circ}C$), and E ($T_{NS} = 1460\,^{\circ}C$) (Figs 11a, b, and c, respectively) shows an average grain size of 0.5, 0.75, and 0.35 μm, respectively. If we define an average grain growth rate as a value determined by dividing the sintered grain size with the corresponding starting particle size over the length of sintering, it can be found a 3 times faster grain growth rate for the powder E than for the powder D and 1.6 times for powder A with respect to powder D, which supports the previous argument. However, competition between grain growth and pore growth frequently exists and can't be ignored, since the latter causes an increase in pore coordination number and should be avoided.

Equation 5 and Fig. 11 strongly suggest that finer particles (e.g., powder E) have a much greater tendency to reduce pore coordination number, suggesting grain growth kinetics dominate. Therefore, a larger pore relative to the particle size (i.e., higher critical ratio) seems kinetically allowable to be present in the fine-powder compacts. Interestingly, powder E is found to have the most extensive agglomeration, the initial densification of the agglomerates may frequently cause an increase in interagglomerate pore size (or increase in pore coordination number). However, the high end-point density suggests these further "opened" interagglomerate pores tend to come back into contact with the matrix by a greater densification force.

Since the critical ratio increases with reducing particle size, by examining Fig. 10, a specific pore size of 0.38 ± 0.08 μm ($\pm$ stands for standard deviation) is obtained by multiplying the critical ratio with the

corresponding particle size. This pore size is believed to be a critical pore dimension, which determines whether the pores in the green compacts can be eliminated, or not. Therefore, current investigation suggested that the pores below the size of about 0.38 μm would be thermodynamically unstable and can be totally eliminated.

4. Conclusion

Fine zirconia powder compacts were prepared from five different powder sources, representing differences in particle size/shape, sinterability, and degree of agglomeration. Average pore diameter has been examined to be a true representative of the whole pore structure in a given powder compact. This pore parameter correlates well with the sintering behaviour of the powder compacts at a variety of sintering stages. A critical pore diameter/particle size ratio has been experimentally determined, which is shown to be inversely proportional to the power-law dependence of the starting particle size; the smaller the particles, the greater value of the ratio is permitting. This is primarily because of the greater tendency for grain growth during sintering. The pore coordination number can be reduced to a significant extent for the smaller particles and this allows further pore elimination at the final stage of sintering. A simple expression for pore stability has been experimentally deduced which is primarily valid for the fine zirconia powders under investigation, with a particle size ranging from 0.08 to 0.5 μm; however, an extend application of this expression to other ceramic system receives an excellent predictive capability.

Acknowledgement

The authors are gratefully indebted to the Minister of Economic Affair, Taiwan ROC for supporting this research work under contract number 863KG2230.

References

1. E. A. BARRINGER and H. K. BOWEN, *J. Amer. Ceram. Soc.* **62**(12) (1982) c199–c201.
2. T. S. YEH and M. D. SACKS, *ibid.* **71**(12) (1988) c484–c487.
3. M. D. SACKS and G. W. SCHEIFFELE, *Ceram. Eng. Sci. Proc.* **6**(7/8) (1985) 1109–1123.
4. W. H. RHODES, *J. Amer. Ceram. Soc.* **64**(1) (1981) 19–22.
5. I. A. AKSAY, F. F. LANGE and B. I. DAVIS, *ibid.* **66**(10) (1983) c190–c192.
6. M. PARISH and H. K. BOWEN, *Ceramics Intern.* **10** (1984) 75–77.
7. H. L. HSIEH and T. T. FANG, *J. Amer. Ceram. Soc.* **73**(6) (1990) 1566–1573.
8. F. DOGAN, A. ROOSEN and H. HAUSNER, *Sci. Ceram.* **13** (1985) c1/231–235.
9. A. ROOSEN and H. HAUSNER, *Adv. Ceram.* **12** (1984) 714–726.
10. A. ROOSEN and H. K. BOWEN, *J. Amer. Ceram. Soc.* **71**(11) (1988) 970–977.
11. D. M. LIU, *Ceramics International*, in press.
12. D. M. LIU and W. J. TSENG, *J. Mater. Sci.*, in press.
13. R. G. FREY and J. W. HALLORAN, *J. Amer. Ceram. Soc.* **67**(3) (1984) 199–203.
14. J. S. REED, T. CARBONE, C. SCOTT and S. LUKASIEWICZ, in "Processing of Crystalline Ceramics," edited by H. Palmour III, R. F. Davis and T. M. Hare (Plenum, New York, 1978) pp. 171–180.
15. C. A. BRUCH, *Amer. Ceram. Soc. Bull.* **41**(12) (1962) 799–806.
16. W. D. KINGERY and B. FRANCOIS, in "Sintering and Related Phenomena," edited by G. C. Kuczynski, N. A. Hooton and C. F. Gibbon (Gordon and Breach, Science Publishers, New York, 1967) pp. 471–498.
17. F. F. LANGE, *J. Amer. Ceram. Soc.* **67**(2) (1984) 83–89.
18. J. ZHENG and J. S. REED, *Amer. Ceram. Soc. Bull.* **71**(9) (1992) 1410–1416.
19. F. F. LANGE, *J. Amer. Ceram. Soc.* **72** (1989) 3–15.
20. J. RODRIGUEZ, C. H. ALLIBERT and J. M. CHAIX, *Powder Technol.* **47** (1986) 25–33.
21. N. M. VISSCHER and M. BOLSTERLI, *Nature* **239** (1972) 504.
22. M. DIXMIER, *J. Physique* **39** (1978) 873.
23. D. M. LIU and C. T. FU, *Ceramics International* **22** (1996) 101–106.
24. F. M. TILLER and C. D. TSAI, *J. Amer. Ceram. Soc.* **69**(12) (1986) 882–887.
25. F. W. DYNYS and J. W. HALLRON, *ibid.* **66**(9) (1984) 596–601.
26. M. D. SACKS and J. A. PASK, *ibid.* **65**(2) (1982) 70–77.
27. J. ZHENG and J. S. REED, *ibid.* **75**(5) (1989) 810–817.
28. D. M. LIU, *J. Mater. Sci. Mater. Med.*, in press.
29. D. M. LIU, *Biomaterials* **17**(20) (1996) 1955–1958.

Received 24 December 1996
and accepted 11 November 1998